

Experimental validation of analytical wake and downstream turbine performance modelling

Felix Polster¹, Jan Bartl², Franz Mühle³, Paul Uwe Thamsen¹ and Lars Sætran²

¹ Chair of Fluid System Dynamics, Technical University of Berlin, Germany

² Department of Energy and Process Engineering, Norwegian University of Science and Technology, Trondheim, Norway

³ Faculty of Environmental Sciences and Natural Resource Management, Norwegian University of Life Sciences, Ås, Norway

E-mail: felix.polster@t-online.de

Abstract. Wake effects in wind farms can cause significant power losses. In order to reduce these losses layout and control optimization can be applied. For this purpose, simple and fast prediction tools for the wake flow are needed. In the first part of this work, five analytical wind turbine wake models are compared to small-scale turbine wind tunnel measurements. The measurements are conducted at several downstream distances, varying the ambient turbulence intensity and upstream turbine blade pitch angle. Furthermore, an adjustment of a recently developed wake model is proposed. Subsequently, the adjusted model is found to perform best throughout all test cases. In the second part, the performance of an aligned downstream turbine is modelled based on the predicted wake flow using a Blade Element Momentum method with guaranteed convergence. In order to consider the non-uniform inflow velocity a mean-blade-element-velocity method is developed. Moreover, a blockage effect correction is applied. A comparison to wind tunnel measurement data shows that the wake velocity as well as the combined power of two aligned turbines are fairly well predicted. Additionally, the presented analytical framework of wake and downstream turbine performance modelling proposes several model improvements for state-of-the art wind farm simulation tools.

1. Introduction

Wake effects in wind farms can cause significant power losses. Average offshore wind farm power losses due to wind turbine wakes are in the range of 10 - 20 % [1]. For low turbine spacing as in case of Lillgrund offshore wind farm power losses can amount up to 23 % [2]. In order to reduce power losses wind farm layout and control optimization can be applied. For this purpose, simple and fast wake modelling tools are needed. One of the pioneering analytical single wake models is the one proposed by N.O. Jensen [3] in 1983. The model is based on conservation of momentum and assumes a uniform velocity profile inside the wake. Furthermore, it includes a constant approximated thrust coefficient. Katic et al. [4] further developed this model in 1986 taking wind turbine characteristics such as a variable thrust coefficient into account. This model is widely known as the Jensen model or PARK model. In 2004, Ishihara et al. [5] developed a wake model, which for the first time takes the effect of turbulence intensity in the wake on the wake recovery into account. Subsequently, in 2006, Frandsen et al. [6] proposed another top-hat shape single wake model for modelling of wind farm efficiencies. A recently developed analytical



Table 1: Overview of wake measurement test cases

Test Case	Upstream Turbine	TSR λ [-]	Pitch β [°]	Ambient turbulence intensity I_a [%]	Downstream distance [D]
A	T3	3.5	0	0.23, 10	2 - 15
B	T1	6	0, 2, 5	10	3, 5, 9

wake model is the one proposed by Bastankah & Porté-Agel [7] in 2014. The model predicts a Gaussian wake shape and is derived by applying mass and momentum conservation. One of the newest analytical wake models is the one proposed by Gao et al. [8] in 2016. It is based on the Jensen model using a Gaussian wake shape. Furthermore, the model includes a new turbulence intensity model, which takes ambient and rotor added turbulence intensity into account.

2. Methods

2.1. Experimental description

All experiments are conducted in the closed-loop wind tunnel at Norwegian University of Science and Technology (NTNU) in Trondheim. The wind tunnel consists of a test section of 2.71 m width, 1.81 m height and 11.15 m length. In this work, the streamwise direction is defined as x , the horizontal spanwise direction as z and the vertical spanwise direction as y . Measurements with three wind turbines of diameters $d_{T1} = 0.944$ m, $d_{T2} = 0.894$ m and $d_{T3} = 0.450$ m are performed. A detailed turbine description is given in Garica et al. [9] and Bartl et al. [10].

The measurements are conducted at two different ambient turbulence intensities, $I_{a,low} = 0.23\%$ and $I_{a,high} = 10\%$. A constant ambient turbulence intensity of $I_{a,low} = 0.23\%$ is reached in the clean wind tunnel without any flow disturbance. It should be noted that this can only occur in wind tunnel facilities. The high ambient turbulence intensity at turbine position is achieved by installing a turbulence grid at the inlet to the test section. By using the turbulence grid a turbulent flow is generated, which decays with downstream distance. This effect is described in detail in [10].

For the wake measurements a two-component laser doppler anemometer (LDA) is utilised. The reference velocity U_{ref} at the test section inlet is kept constant at 11.5 m/s during all measurements. Furthermore, air temperature as well as ambient pressure are measured consistently to compute the air density. In total, two comprehensive wake measurement series are conducted. Test case A represents wake measurements behind turbine T3 at all integer downstream distances in the range of $x/D = 2$ to $x/D = 15$, applying two different ambient turbulence intensities. Test case B describes wake measurements behind turbine T1 at downstream distances $x/D = 3, 5$ and 9 at three upstream turbine blade pitch angles, $\beta = 0^\circ, 2^\circ$ and 5° . An overview is given in table 1.

In order to compute the mechanical power output, the wind turbine torque T and rotational speed n are measured continuously on the rotor shaft. Additionally, the thrust force F is measured using a six-component force balance. Performance measurements of two aligned turbines, upstream (T1) and downstream (T2) turbine, are conducted at downstream turbine locations $x/D = 3, 5$ and 9 . The ambient turbulence intensity is kept constant at $I_a = 10\%$. Furthermore, no upstream blade pitch is applied, $\beta = 0^\circ$.

2.2. Comparison methods

To assess the wake models ability to predict the measured wakes, two different methods are applied in this work. The mean absolute percentage error (MAPE) is a widely used error

measure that compares measured and modelled variables and computes an absolute mean error in percent. For its calculation all measured velocities U_m are compared to the predicted velocities U_p at the exact same location in horizontal (z) direction. The overline represents an average over all the data points.

$$MAPE = \frac{\overline{|U_m - U_p|}}{\overline{|U_m|}} \cdot 100. \quad (1)$$

The available power percentage error (APPE) is a newly developed method. It compares the measured and modelled available power in the wind for extraction by a downstream turbine. In order to compute the available power for a downstream turbine, the average velocity in the wake between $-R_0 < z < R_0$, where R_0 is the rotor radius, is calculated and subsequently cubed

$$APPE = \frac{\overline{U_m^3} - \overline{U_p^3}}{\overline{U_m^3}} \cdot 100, \quad -R_0 < z < R_0. \quad (2)$$

2.3. Blockage correction

In small-scale wind tunnel measurements blockage effects can be observed. It describes the condition, in which air flow in the wind tunnel is partially blocked by the wind turbine rotor area. The aim of blockage effect correction is to determine the corrected inflow velocity. In the present study the blockage effect correction method proposed by Ryi et al. [11] based on the one-dimensional momentum approach of Glauert is used. By applying one-dimensional axial momentum theory Ryi et al. developed a set of six equations, described in detail in [11]. Knowing the blockage ratio and measuring or simulating the thrust, six unknowns remain and the corrected velocity can easily be computed. Consequently, the corrected power coefficient, thrust coefficient and tip speed ratio are

$$C_{P,cor} = C_P \left(\frac{U_{cor}}{U_{ref}} \right)^3, \quad C_{T,cor} = C_T \left(\frac{U_{cor}}{U_{ref}} \right)^2, \quad \lambda_{cor} = \lambda \left(\frac{U_{cor}}{U_{ref}} \right), \quad (3)$$

where U_{cor}/U_{ref} is the blockage effect correction factor. It should be noted, that in this work the modelled and not the measured values are corrected. Eventually, the corrected wake velocity computed by the wake models is

$$U_{new} = U \left(\frac{U_{cor}}{U_{ref}} \right). \quad (4)$$

2.4. Wake models

The Jensen wake model is based on conservation of momentum. It further assumes a uniform velocity profile and a linear expanding wake. The normalized wake velocity and wake width D_w as a function of downstream distance x are

$$\frac{U(x)}{U_{ref}} = 1 - \frac{1 - \sqrt{1 - C_T}}{(1 + 2kx/D_0)^2}, \quad D_w(x) = 2kx + D_0, \quad (5)$$

where k is the wake decay constant and D_0 is the rotor diameter. According to N.O. Jensen this value is constant and approximately 0.1 [3]. However, detailed subsequent investigations found the wake decay constant to be a function of surface roughness and thus the ambient turbulence intensity [12]. Therefore, the widely used correlation from WindPRO is applied in this work [13]

$$k \approx 0.5I_a. \quad (6)$$

The Ishihara wake model is based on momentum conservation, a two-dimensional axisymmetric flow and a self-similar wake. It further takes the influence of ambient and rotor

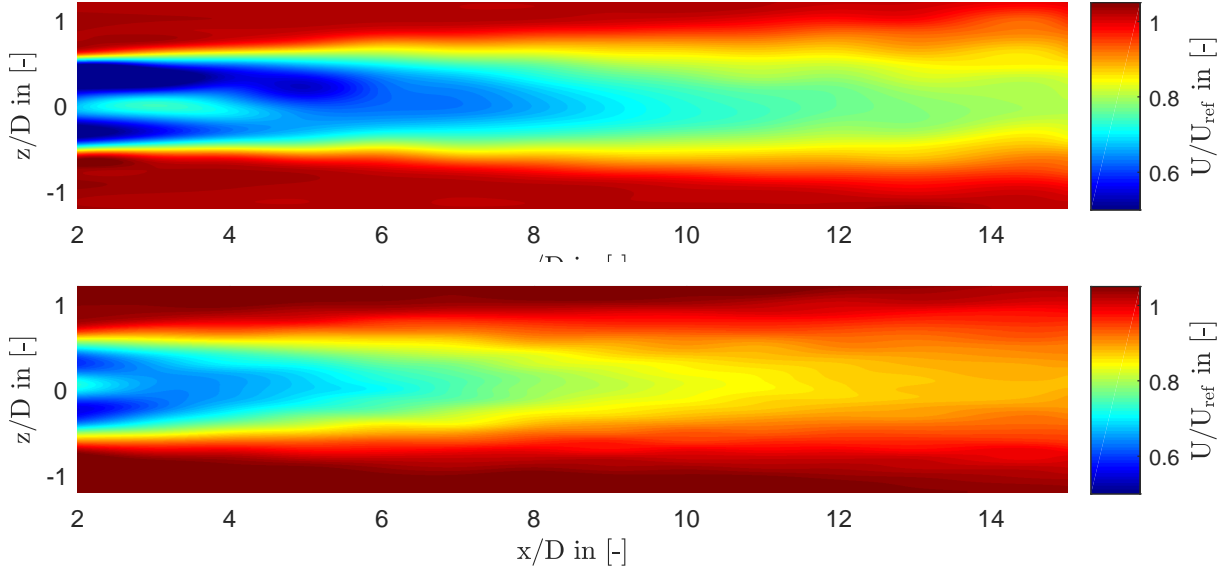


Figure 1: Test case A: Wake measurement results at hub height at **(top:)** $I_{a,low} = 0.23\%$, **(bottom:)** $I_{a,high} = 10\%$ at downstream distances $x/D = 2 - 15$

added turbulence intensity on the wake recovery p into account. The normalized velocity, the wake width b , wake recovery and mechanical generated turbulence intensity I_w are

$$\frac{U(x, r)}{U_{ref}} = \frac{C_T^{0.5}}{32} \left(\frac{1.666}{k_1} \right)^2 \left(\frac{x}{D_0} \right)^{-p} \exp \left(-\frac{r^2}{b^2} \right), \quad (7)$$

$$b(x) = \frac{k_1 C_T^{0.25}}{0.833} D_0^{1-\frac{p}{2}} x^{\frac{p}{2}}, \quad (8)$$

$$p = k_2 (I_a + I_w), \quad (9)$$

$$I_w = \begin{cases} k_3 \frac{C_T}{I_a} \left(1 - \exp \left(-4 \left(\frac{x}{10D_0} \right)^2 \right) \right) & , I_a > 0.03 \\ k_3 \frac{C_T}{0.03} \left(1 - \exp \left(-4 \left(\frac{x}{10D_0} \right)^2 \right) \right) & , I_a \leq 0.03. \end{cases} \quad (10)$$

Frandsen derived his model by applying mass and momentum conservation to a control volume around the turbine. Same as the Jensen wake model, it further assumes a uniform velocity profile inside the wake. The velocity profile and the wake width can be described by

$$\frac{U(x)}{U_{ref}} = 1 - \left(\frac{1}{2} \left(1 - \sqrt{1 - 2 \frac{A_0}{A_w} C_T} \right) \right), \quad D_w(x) = \left(\beta + \frac{\alpha x}{D_0} \right)^{\frac{1}{2}} D_0, \quad (11)$$

with

$$\beta = \frac{1 + \sqrt{1 - C_T}}{2\sqrt{1 - C_T}}. \quad (12)$$

The expansion factor α can be expressed as a function of the wake decay constant and is in order of $\alpha = 10k$, where k is the wake decay coefficient from equation (6).

The Bastankah & Porté-Agel model wake model is derived by applying mass and momentum conservation. Additionally, viscous and pressure terms are neglected in the momentum equation and a self-similar wake with Gaussian shape is assumed. Similar to the Jensen model the wake is

expected to expand linearly with a growth rate k^* . The normalized wake velocity as a function of the streamwise and spanwise directions x, y, z is

$$\frac{U(x, y, z)}{U_{\text{ref}}} = 1 - \left(1 - \sqrt{1 - \frac{C_T}{8(k^*x/D_0 + \epsilon)^2}}\right) \exp\left(\frac{-1}{2(k^*x/D_0 + \epsilon)^2} \left(\frac{z - z_h}{D_0}\right)^2 + \left(\frac{y}{D_0}\right)^2\right), \quad (13)$$

with $\epsilon = 0.2\sqrt{\beta}$. Subsequently, based on LES results Niayfar & Porté-Agel [14] found the wake growth rate to be $k^* = 0.3837I + 0.003678$, applicable in the range of $6.5\% < I_a < 15\%$.

The Jensen-Gaussian wake model (JGWM) combines the Jensen model velocity deficit calculation with an Gaussian wake shape. Based on three assumptions, which are described in detail in [8] the normalized velocity can be calculated as

$$\frac{U(x, r)}{U_{\text{ref}}} = 1 - (1 - U_c(x)) \frac{5.16}{\sqrt{2\pi}} \exp\left(\frac{-r^2}{(k'x + R_0)^2 / 3.3282}\right), \quad (14)$$

where U_c is equal to the one computed by the Jensen model (5).

$$U_c(x) = 1 - \frac{1 - \sqrt{1 - C_T}}{(1 + 2k'x/D_0)^2}, \quad (15)$$

where k' is the modified wake decay constant. It is a function of the ambient and the rotor added turbulence intensity. Tian et al. [15] proposed the following correlation between the two wake decay constants

$$k' = k \frac{I_{\text{wake}}}{I_a}, \quad (16)$$

where I_{wake} is the turbulence intensity inside the wake at a certain downstream distance. Gao et al. proposed an own empirical engineering model to compute this value.

$$I_{\text{wake,Gao}} = \left(0.4 \frac{C_T}{(x/D_0)^{0.5}} + I_a^{0.5}\right)^2. \quad (17)$$

However, further investigations of the JGWM found a strong sensitivity to the applied turbulence intensity model. The Crespo and Hernandez turbulence intensity model [16] was found to give a significantly better wake prediction. Therefore, the adjusted JGWM will be used in the following.

$$I_+ = 0.73a^{0.8325} I_a^{0.0325} (x/D_0)^{-0.32}, \quad (18)$$

$$I_{\text{wake,C\&H}} = \sqrt{I_a^2 + I_+^2}. \quad (19)$$

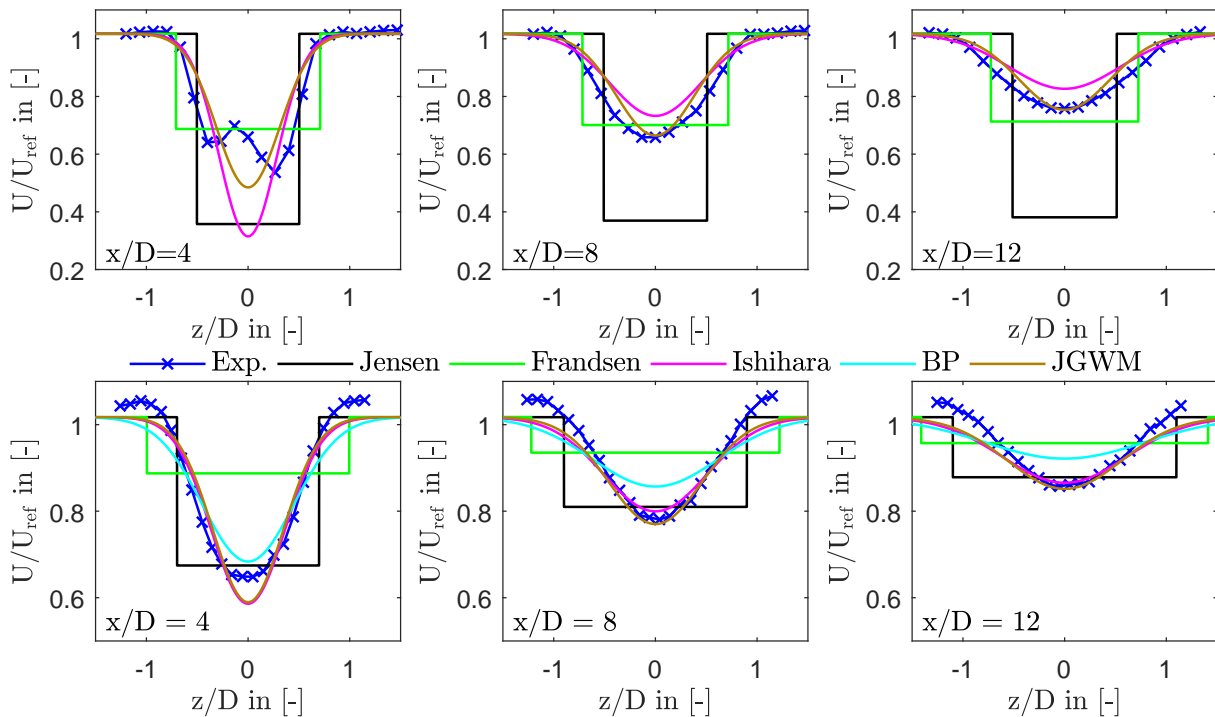
where I_+ is the rotor added turbulence intensity and a is the axial induction factor, which is defined as the ration between axial velocity deficit at the rotor plane and free stream velocity.

2.5. Velocity calculation methods

A Blade Element Momentum solution method with guaranteed convergence by S.Ning [17] is used to model power output and thrust force of the upstream and downstream turbine. In order to model the downstream turbine performance the predicted wake velocities from the analytical models are utilised. Furthermore, two different velocity calculation methods are applied to determine the inflow velocity at the downstream rotor area. The simple mean-rotor-velocity (MRV) method calculates an average velocity over the rotor swept area. The mean-blade-element-velocity method computes a mean velocity for each blade element. Subsequently, this mean velocity is used as the inflow wind speed for that specific blade element. Both methods are applied and compared in the next section.

Table 2: Test case A: Wake prediction results using the comparison methods MAPE and absolute APPE averaged over downstream distances $x/D = 2 - 15$ at two ambient turbulence intensities

	$I_a = 0.23\%$		$I_a = 10\%$	
	MAPE [%]	APPE [%]	MAPE [%]	APPE [%]
Jensen	19.6	84.7	6.8	6.7
Frandsen	8.4	29.5	10.3	60.1
Ishihara	7.3	28.9	3.8	6.5
BP	-	-	5.3	20.2
JGWM	5.2	11.2	3.4	3.3

Figure 2: Test case A: Wake measurement and modelling results at hub height at **(top:)** $I_{a,low} = 0.23\%$ and **(bottom:)** $I_{a,high} = 10\%$ and downstream distances $x/D = 4, 8, 12$

3. Results and discussion

3.1. Wake prediction: Test Case A

Test case A represents wake measurements at ambient turbulence intensities $I_{a,low} = 0.23\%$ and $I_{a,high} = 10\%$ and a fixed blade pitch angle of $\beta = 0^\circ$. The measured thrust coefficient at design TSR is 0.8847, which results in a blockage effect correction factor of 1.0173. The measurement results are given in Figure 1. A two dimensional spline interpolation is applied in order to compute the approximate values in between the measured values. Figure 2 shows the corresponding measured and predicted line wakes at downstream distances $x/D = 4, 8$ and 12 . The resulting MAPE and APPE averaged over all downstream distances are given in Table 2.

At $I_a = 0.23\%$ the Jensen model shows no wake recovery or wake expansion at all. This is caused by the small wake decay constant of 0.0012, calculated using equation (6). Therefore, the Jensen model is not applicable at low ambient turbulence intensities. At $I_a = 10\%$ the Jensen

wake model performs significantly better. Centerline velocity as well as wake expansion are well predicted due to a realistic wake decay constant of 0.05. Consequently, a MAPE and APPE of only 6.8% and 6.7% are achieved, respectively. The Frandsen model is characterized by an underestimation of the wake recovery rate at $I_a = 0.23\%$. At $I_a = 10\%$ the centerline velocity is significantly overestimated at all downstream distances. This observation is in accordance with full-scale turbine LES comparisons at different surface roughnesses [7]. Consequently, MAPE and APPE values represent an inaccurate wake prediction. At $I_a = 0.23\%$ the Ishihara model shows reasonable agreement with the measurements. In particular, the wake expansion is well predicted, whereas the wake recovery rate is overestimated by the wake model. At $I_a = 10\%$ the model gives an accurate wake prediction, which is represented by a MAPE of 3.8% and APPE of 6.5%, respectively. Particularly, in the far wake from $x/D = 8$ the centerline velocity is almost perfectly modelled. The BP model is only defined at ambient turbulence intensities between 6.5% and 15%. At $I_a = 10\%$ the wake velocity prediction is characterized by a strong overestimation. Especially, in the wake center. Therefore, the model yields an high APPE of 20%, which represents an inaccurate wake prediction. The adjusted Jensen-Gaussian wake model shows a very good agreement with the measurements at both ambient turbulence intensities. Particularly, in the far wake the centerline velocity is perfectly predicted at all downstream distances. Consequently, very low values for MAPE and APPE are achieved. Therefore, the adjusted JGWM is a robust analytical wake model in terms of a ambient turbulence intensity variation. It should be noted again, that applying the initial Gao turbulence intensity model yields a significantly lower prediction accuracy.

3.2. Wake prediction: Test Case B

Wake measurements are conducted at pitch angles $\beta = 0^\circ$, 2° and 5° , while the ambient turbulence intensity is kept constant at 10%. The associated thrust coefficients determined by measurements are 0.8497, 0.6944 and 0.517, respectively. This results in blockage correction factors of 1.0525, 1.0373 and 1.0243, respectively. The measurement and modelling results are given in Figure 3 as line wakes at $x/D = 3, 5$ and 9. Since all wake models are unable to predict the double-Gaussian wake shape, the models are mainly evaluated using the available power comparison method APPE, which is given in Table 3.

Increasing the blade pitch angle away from the design point $\beta = 0^\circ$ reduces the angle of attack. Therefore, the blade lift decreases, whereas the drag increases. Consequently, the power output and rotor thrust decrease, which results in a higher wake velocity behind the turbine. In general, all wake models are able to predict this effect. In particular, the Jensen model and the adjusted JGWM show a high sensitivity to a change of the rotor thrust. Both models give an accurate wake flow prediction of the available power in the wake at all blade pitch angles and downstream distances. Consequently, a reasonable APPE of 12% for the Jensen model and 8.2% for the adjusted JGWM are achieved. Contrarily, the Frandsen model and BP model are characterized by a low sensitivity to a change of rotor thrust. Additionally, the Frandsen model overestimates the wake velocity at all blade pitch angles and downstream distances. Same applies for the BP model at downstream distance $x/D = 9$. The Ishihara model also reacts insufficiently to blade pitch angle variation. However, the predicted wake is always roughly in magnitude of the measurements. Therefore, the absolute average APPE amounts 15.3%, which is a reasonable result.

In total, the adjusted JGWM is the most accurate wake at all inflow conditions, pitch angles and downstream distances. Therefore, it is used in the following section to predict the power output of a downstream turbine.

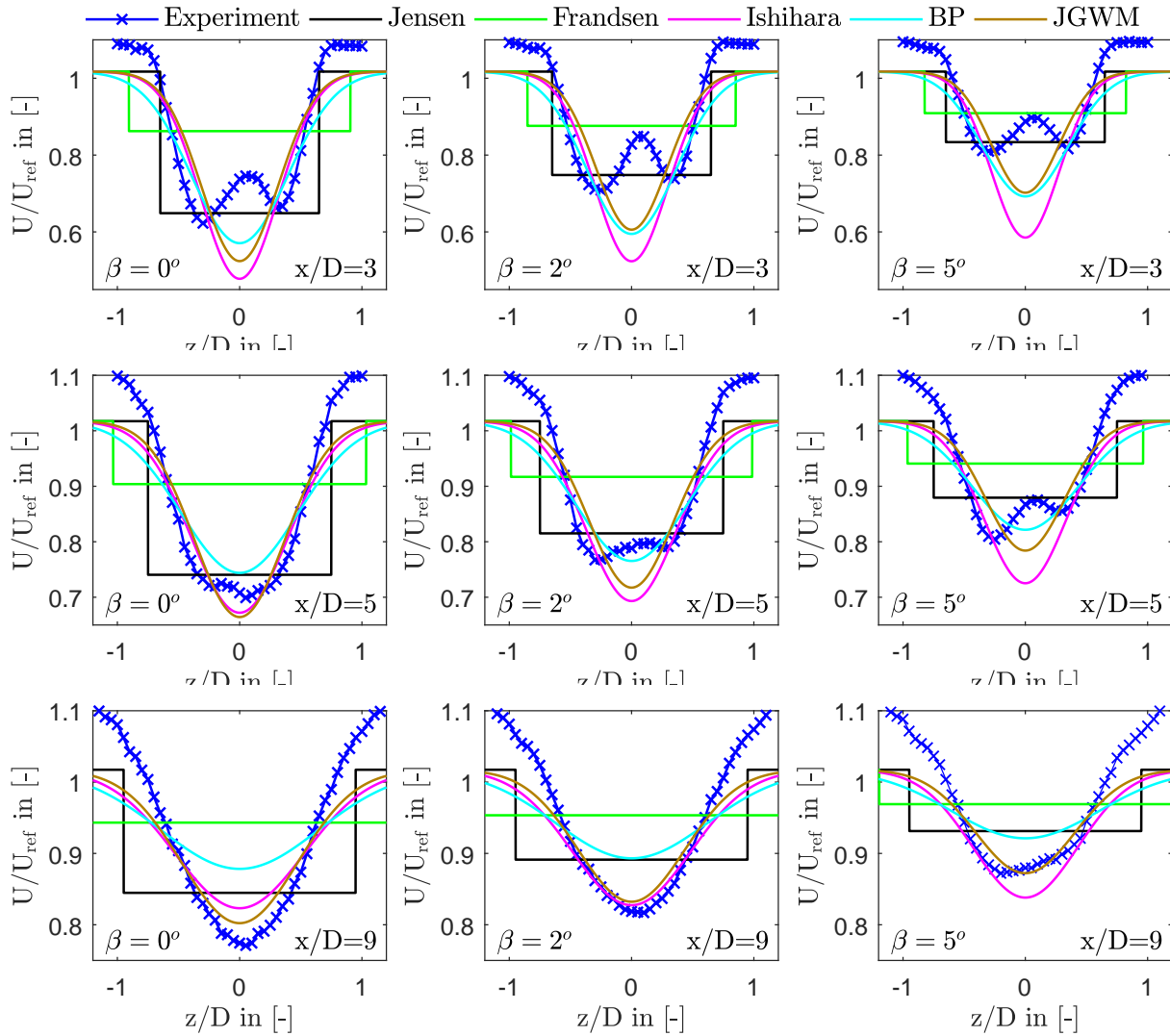


Figure 3: Test case B: Wake measurement and modelling results at hub height at blade pitch angles $\beta = 0^\circ, 2^\circ, 5^\circ$ and downstream distances $x/D = 3, 5, 9$

Table 3: Test case B: Absolute averaged wake prediction results using the comparison methods MAPE and APPE at all blade pitch angles and downstream distances

	MAPE [%]	APPE [%]
Jensen	6.6	12.0
Frandsen	12.5	57.2
Ishihara	6.6	15.3
BP	7.1	19.3
JGWM	5.9	8.2

3.3. Performance prediction

The upstream power and thrust measurement and modelling results are given in Figure 4 and Table 4. In order to underline the necessity of blockage on the turbine performance the non-

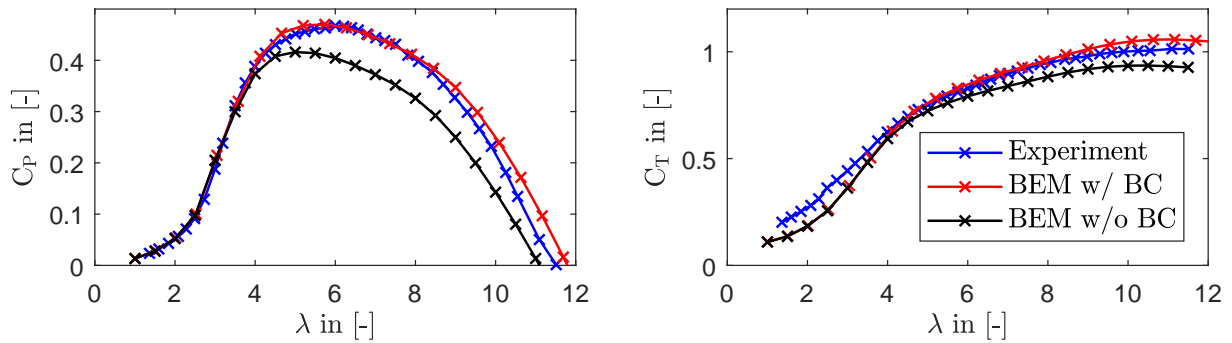


Figure 4: Upstream turbine performance coefficients with and without blockage effect correction at blade pitch angle $\beta = 0^\circ$ and $I_{a,high} = 10\%$

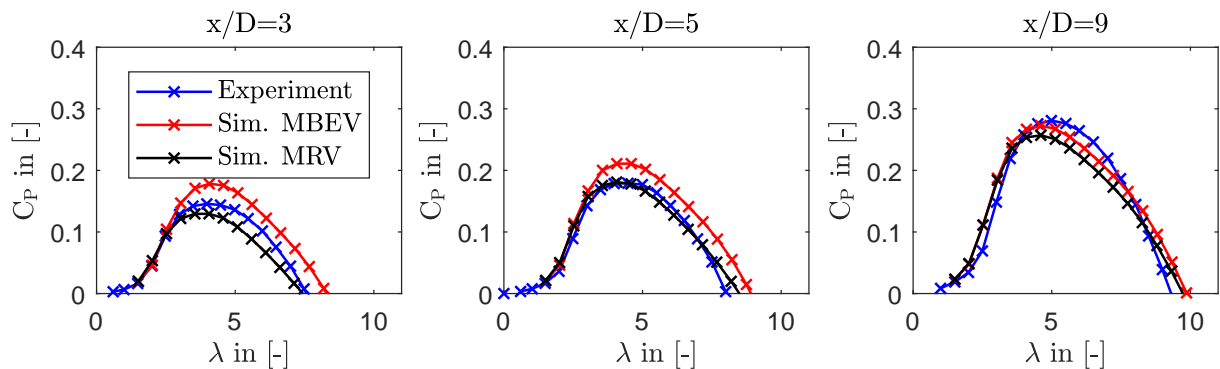


Figure 5: Downstream turbine power coefficients using the mean-blade-element-velocity (MBEV) and mean-rotor-velocity (MRV) methods

Table 4: Upstream and downstream turbine performance at operating tip speed ratio $\lambda_{down} = 4.5$

	$C_{T,up}$ in [-]	$C_{P,up}$ in [-]	$C_{P,down}$ in [-]		
			$x/D = 3$	$x/D = 5$	$x/D = 9$
Experiment	0.828	0.467	0.143	0.179	0.276
Simulation MBEV	0.848	0.468	0.177	0.212	0.272
Simulation MRV	0.848	0.468	0.124	0.179	0.257

corrected thrust and power coefficients are displayed as well. Generally, the BEM method with blockage effect correction gives a very accurate performance prediction. The measured power coefficient at design tip speed ratio $\lambda_D = 6$ amounts 0.467. Whereas, the modelled power coefficient corrected by the blockage model is 0.468. The resulting prediction error of 0.2% represents a very accurate power prediction. Same applies for the thrust coefficient, where the prediction error amounts 2.4%.

In order to model the downstream turbine performance, at first, the upstream turbine thrust coefficient is modelled. Subsequently, a blockage effect correction is applied. The corrected thrust coefficient is then used as input parameter to the adjusted Jensen-Gaussian wake model. Subsequently, the two velocity calculation methods MRV and MBEV are applied to predict the downstream turbine power. Finally, a blockage effect correction is applied to the downstream turbine. The resulting measured and predicted power coefficients are displayed in Figure 5

and given in Table 4. The MRV method is characterized by a slight underestimation of the downstream turbine power. However, the averaged percentage prediction error at all downstream distances amounts only 6.7%. Particularly, at $x/D = 5$ the power output is perfectly predicted. Contrarily, the MBEV method is characterized by an overestimation of the downstream turbine power. In particular, at downstream distances $x/D = 3$ and $x/D = 5$. Consequently, the averaged percentage prediction error amounts 14.6%.

In general, the downstream turbine performance predictions are performing fairly well considering the complex wake flow they are exposed to. However, a lower prediction accuracy can be observed modelling the downstream turbine power. This is caused by additional prediction uncertainties due to the wake prediction.

4. Conclusions

Five analytical wind turbine wake models were compared to wind tunnel measurements. Thereby, the models' sensitivity to ambient turbulence intensity and rotor thrust was investigated. The Frandsen model was found to be unable to predict the wake velocities reasonably at all test cases. The Bastankah & Porté-Agel model gave a better wake prediction. However, due to an overestimation of the wake velocity, still high prediction errors were identified. The Ishihara model was found to predict the measured wake velocity accurately at high ambient turbulence intensity and non-pitched blades. However, the model showed a insensitivity towards a change of rotor thrust. Conversely, the Jensen model revealed a high and sufficient sensitivity to rotor thrust variation. Furthermore, it gave an accurate prediction at high ambient turbulence intensity. Additionally, the model was found not to be applicable at low ambient turbulence intensities. An adjustment of a recently developed wake model, the Jensen-Gaussian wake model was performed. Eventually, the model was found to give the best overall wake flow prediction. Subsequently, this model was applied on performance modelling of a downstream turbine using a Blade Element Momentum method with guaranteed convergence. Furthermore, two velocity-calculation methods were compared to predict the downstream turbine power. In general, upstream power as well as thrust coefficient were very accurately predicted. The downstream turbine performance was found to be fairly well predicted using the mean-rotor-velocity method. Consequently, the averaged combined power output prediction error at all downstream distances amounts only 1.8%. Using the mean-blade-element-velocity method resulted in a slightly higher prediction error. In summary, the adjusted Jensen-Gaussian wake model and the mean-rotor-velocity method are recommended for application in wind farm modelling.

References

- [1] Barthelmie R J, Hansen K, Frandsen S T, Rathmann O, Schepers J, Schlez W, Phillips J, Rados K, Zervos A, Politis E *et al.* 2009 *Wind Energy* **12** 431–444
- [2] Barthelmie R J, Pryor S, Frandsen S T, Hansen K S, Schepers J, Rados K, Schlez W, Neubert A, Jensen L and Neckelmann S 2010 *Journal of Atmospheric and Oceanic Technology* **27** 1302–1317
- [3] Jensen N O 1983 *A note on wind generator interaction*
- [4] Katic I, Højstrup J and Jensen N O 1986 407–410
- [5] Ishihara T, Yamaguchi A and Fujino Y 2004 Development of a new wake model based on a wind tunnel experiment Tech. rep. Global Wind
- [6] Frandsen S, Barthelmie R, Pryor S, Rathmann O, Larsen S, Højstrup J and Thøgersen M 2006 *Wind energy* **9** 39–53
- [7] Bastankhah M and Porté-Agel F 2014 *Renewable Energy* **70** 116–123
- [8] Gao X, Yang H and Lu L 2016 *Applied Energy* **174** 192–200
- [9] Garcia L, Vatn M, Mühle F and Sætran L 2017 Experiments in the wind turbine far wake for the evaluation of an analytical wake model *Journal of Physics: Conference Series* vol 854 (IOP Publishing) p 012015
- [10] Bartl J and Sætran L 2017 *Wind Energy Science* **2** 55–76
- [11] Ryi J, Rhee W, Hwang U C and Choi J S 2015 *Renewable Energy* **79** 227–235

- [12] Peña A, Réthoré P E and Laan M P 2015 *Wind Energy*
- [13] Nielsen P 2010 *EMD International A/S*
- [14] Niayifar A and Porté-Agel F 2016 *Energies* **9** 741
- [15] Tian L, Zhu W, Shen W, Zhao N and Shen Z 2015 *Journal of Wind Engineering and Industrial Aerodynamics* **137** 90–99
- [16] Crespo A, Herna J *et al.* 1996 *Journal of wind engineering and industrial aerodynamics* **61** 71–85
- [17] Ning S A 2014 *Wind Energy* **17** 1327–1345